

# Boosting Speech Recognition Robustness to Modality-Distortion with Contrast-Augmented Prompts

Anonymous Authors

## ABSTRACT

In the burgeoning field of Audio-Visual Speech Recognition (AVSR), extant research has predominantly concentrated on the training paradigms tailored for high-quality resources. However, owing to the challenges inherent in real-world data collection, audio-visual data are frequently affected by modality-distortion, which encompasses audio-visual asynchrony, video noise and audio noise. The recognition accuracy of existing AVSR method is significantly compromised when multiple modality-distortion coexist in low-resource data. In light of the above challenges, we propose PCD: *cluster-Prompt with Contrastive Decomposition*, a robust framework for modality-distortion speech recognition, specifically devised to transpose the pre-trained knowledge from high-resource domain to the targeted domain by leveraging contrast-augmented prompts. In contrast to previous studies, we take into consideration the possibility of various types of distortion in both the audio and visual modalities. Concretely, we design bespoke prompts to delineate each modality-distortion, guiding the model to achieve speech recognition applicable to various distortion scenarios with quite few learnable parameters. To materialize the prompt mechanism, we employ multiple cluster-based strategies that better suits the pre-trained audio-visual model. Additionally, we design a contrastive decomposition mechanism to restrict the explicit relationships among various modality conditions, given their shared task knowledge and disparate modality priors. Extensive results on LRS2 dataset demonstrate that PCD achieves state-of-the-art performance for audio-visual speech recognition under the constraints of distorted resources.

## CCS CONCEPTS

• **Computing methodologies** → **Speech recognition**; *Computer vision tasks*.

## KEYWORDS

multi-modal learning, audio-visual speech recognition, modality-distortion

## 1 INTRODUCTION

Audio-Visual Speech Recognition (AVSR), which leverages the synergistic interaction between human speech and temporally aligned lip movement videos to generate natural language, has emerged

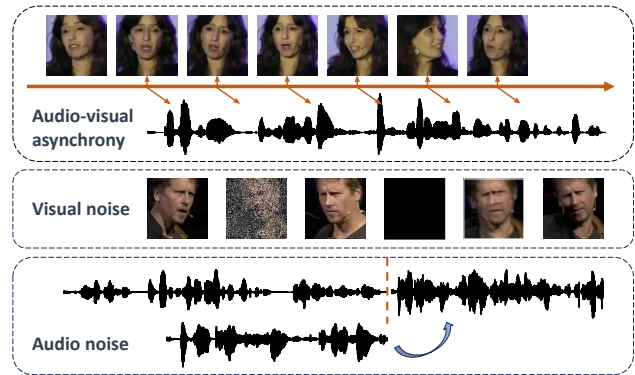


**Figure 1: Examples of potential distortion in audio-visual datasets. Audio-visual asynchrony: the audio and video are out of sync temporally or mismatched across different segments; Visual noise: the video is disturbed by blackouts, blurriness, frame drops, or screen flickering; Audio noise: the audio contains environmental noise.**

as a vibrant frontier in the applications of multi-modal learning [1, 19, 20, 27]. With learning audio-visual features, AVSR has demonstrated superior performance compared to single-modality input models (including audio-only and visual-only input models). While the complementarity of audio and visual modalities is often assumed, the reality frequently deviates from this ideal scenario due to recording equipment and environmental constraints. Instances where data is distorted, such as audio-visual asynchrony induced by storage device malfunctions, audio noise in outdoor interview scenes, or visual noise in video conferencing scenarios (as shown in Fig. 1), often result in the confusion of AVSR model. With modality-distortion, models may even fall short in effectiveness compared to their single-modal counterparts, especially given the presence of multiple distortion scenarios. On the other hand, distorted data can possess inherent value due to the challenges associated with acquiring high-resource datasets and the high cost of label annotation, particularly evident in endeavors such as the preservation of minority languages or data recovery. The ubiquitous presence of distortion in real-life scenarios poses substantial challenges to the application of AVSR.

Established AVSR models are typically trained on high-resource datasets, with the objective of attaining peak performance under circumstances of data completeness or in scenarios where one modality exhibits incompleteness. For instance, numerous AVSR investigations [2, 19, 28, 36] evaluate the efficacy of models amidst audio noise, thereby validating methodological robustness. Currently, alternative research endeavors [4, 5, 10] concentrate on addressing issues pertaining to visual modality missing or noisy.

Permission to make digital or hard copies of all or part of this work for personal or professional use, not for profit or commercial advantage and that copies bear this notice and the full citation on the first page. Copyrights for components of this work owned by others than the author(s) must be honored. Abstracting with credit is permitted. To copy otherwise, or to publish, to post on servers or to redistribute to lists, requires prior specific permission and/or a fee. Request permissions from [permissions@acm.org](mailto:permissions@acm.org).

ACM MM, 2024, Melbourne, Australia

© 2024 Copyright held by the owner/author(s). Publication rights licensed to ACM.

ACM ISBN 978-x-xxxx-xxxx-x/YY/MM

<https://doi.org/10.1145/nnnnnnn.nnnnnn>

117 However, none of these methods address the challenge of training  
 118 with low-quality datasets containing simultaneous audio and  
 119 visual modality-distortion which are commonly encountered in  
 120 real-life situations, lacking robustness across diverse distortion  
 121 scenarios. Training a separate optimal model for each potential  
 122 distortion scenarios is ideal but impractical, given the substantial  
 123 computational resources required. Constrained by the availability  
 124 of high-quality datasets, there is a need for more robust approaches  
 125 that consume fewer computational resources to adapt to data with  
 126 modality-distortion.

127 Incorporating three real-world concerns into consideration: (i)  
 128 distortion occurrences are always diverse and scattered across vari-  
 129 ous modalities; (ii) distortion often stems from equipment and en-  
 130 vironment limitations, hence the distortion forms within the same  
 131 batch of data may be unique and uniform, limited to a single modal-  
 132 ity; (iii) in scenarios where both modalities suffer from severe distor-  
 133 tion, the data is chaotic and devoid of value, leading to confusion in  
 134 model even human recognition. Thereby, we introduce a general set-  
 135 ting to simulate real-world modality-distortion, where the dataset  
 136 comprises three types of scenarios: clean data, data with audio dis-  
 137 tortion, and data with visual distortion. We propose a novel method  
 138 called PCD: Cluster-Prompt with Contrastive Decomposition to  
 139 enhance speech recognition robustness across diverse modality-  
 140 distortion conditions within a unified framework. Drawing inspira-  
 141 tion from the notable success of prompt learning within the field  
 142 of multi-task fine-tuning in natural language processing [8, 18, 37],  
 143 we design tailored prompts for each modality-distortion conditions  
 144 instead of training individual model with a myriad of parameters.  
 145 Building upon a fully pre-trained transformer-based model with  
 146 audio-visual alignment [27], we effectively utilize prompts to facil-  
 147 itate the transfer of knowledge from a pre-trained high resource  
 148 domain to a low-quality domain with modality-distortion. In order  
 149 to enhance compatibility with pre-trained models, we develop  
 150 a cluster module and explore two attachment strategies. Follow-  
 151 ing the computation of features by the cluster module, generated  
 152 prompts are then combined with either the input or key&value  
 153 during multi-head self-attention operations. Furthermore, we em-  
 154 ploy low-rank decomposition and contrastive regularization term,  
 155 supervising the task-specific part of cluster-prompts to provide  
 156 more refined guidance tailored to particular scenarios. Under the  
 157 explicit constraint of task interaction, the modality-distortion tasks  
 158 prompts tends to approach the clean task prompts while diverg-  
 159 ing from each other, allowing prompts to learn more task-relevant  
 160 features. The main contributions are as follows:

- 161 • We propose a novel framework, PCD, which is the first work  
 162 dedicated to enhancing robustness in modality-distortion  
 163 speech recognition.
- 164 • We introduce two cluster-based strategies tailored for im-  
 165 plementing the prompt mechanism, which are especially  
 166 optimized to complement pre-trained audio-visual models.
- 167 • We design a novel contrastive decomposition mechanism for  
 168 prompts, aiming to mine the interactions between diverse  
 169 modality-distortion conditions.
- 170 • PCD achieves the state-of-the-art performance on the LRS2  
 171 dataset, demonstrating its outstanding efficacy in AVSR tasks  
 172 involving modality-distortion.

## 175 2 RELATED WORK 176

### 177 2.1 Audio-Visual Speech Recognition 178

179 Recently, AVSR which aims to translates synchronized audio and  
 180 video into corresponding text, has been attracting increasing re-  
 181 search interest as it presents a viable solution for employing the  
 182 fusion of audio and visual modalities as an alternative to ASR[21,  
 183 23, 26]. TM-seq2seq [1] first introduce transformer architecture  
 184 into AVSR task, utilizing pre-computed visual features and audio  
 185 Log-Mel filter features as inputs. E2E Conformer [20] leverages  
 186 Conformer architectures [7] to extract visual and audio features,  
 187 facilitating end-to-end training. Moreover, LUSL-AVSR [22] uti-  
 188 lize self-supervised learning for AVSR task by incorporating the  
 189 pre-trained model trained in massive unlabelled single modality  
 190 data. Similarly employing self-supervised learning, AV-HuBERT  
 191 [27] learns the correspondence of audio and video modalities by  
 192 masking multi-stream video input and predicts automatically dis-  
 193 covered and iteratively refined multi-modal hidden units. Recently,  
 194 Auto-AVSR [19] effectively expand the audio-visual dataset by uti-  
 195 lizing pre-trained ASR models to automatically transcribe unlabeled  
 196 video data.

197 Typically, AVSR research leverages the visual modality to en-  
 198 hance robustness against audio noise [16, 17, 28, 34], while some  
 199 studies also address potential video noise in audio-visual dataset.  
 200 [3, 4] tackles scenarios with missing video frames, while [9] fo-  
 201 cuses on resolving occlusions that may occur in videos. However,  
 202 the aforementioned methodologies only address a singular type  
 203 of distortion, thus lacking robustness across diverse scenarios. In  
 204 contrast, this paper conducts a more thorough study on AVSR's  
 205 robustness where various modality-distortion would occur for any  
 206 data sample and anywhere in learning phases, particularly focusing  
 207 on reducing the computation of model fine-tuning.

### 208 2.2 Prompt Learning 209

210 In prompt-driven approaches, task-specific textual descriptions or  
 211 cues are utilized to guide models towards integrating and concu-  
 212 rrently processing data originating from various sensors, sources,  
 213 or formats such as text, images, audio, or video [6, 14, 18]. This  
 214 methodology has found extensive usage within the field of natural  
 215 language processing and has recently been introduced into vision  
 216 problems [12, 33, 38], audio generation [11, 32] and multi-modal  
 217 learning tasks[35, 40]. [15, 25] introduce prefix tuning, exploring  
 218 additional interactions between prompts and pre-trained model.  
 219 [14, 31, 39] fine-tune pre-trained models by optimizing continuous  
 220 set of prompt vectors called soft prompt instead of hand-crafted  
 221 prompts. In multi-modal tasks, MaPLe [13] applies prompts in both  
 222 vision and language encoders to improve the alignment between  
 223 vision and language representation. TRIPLET [24] further employs  
 224 decoupled prompts and prompt interaction strategies to capture the  
 225 complex interactions between modalities. These studies investigate  
 226 the remarkable adaptability of prompt learning across various tasks  
 227 involving diverse input domains. Inspired by the aforementioned  
 228 work, we introduce prompt learning into AVSR task, transferring  
 229 knowledge from high-resource domains to target domains contain-  
 230 ing various types of modality-distortion which can be regarded  
 231 as different learning tasks. We further experiment with various  
 232 prompt strategies to better align with the pre-trained AVSR model.

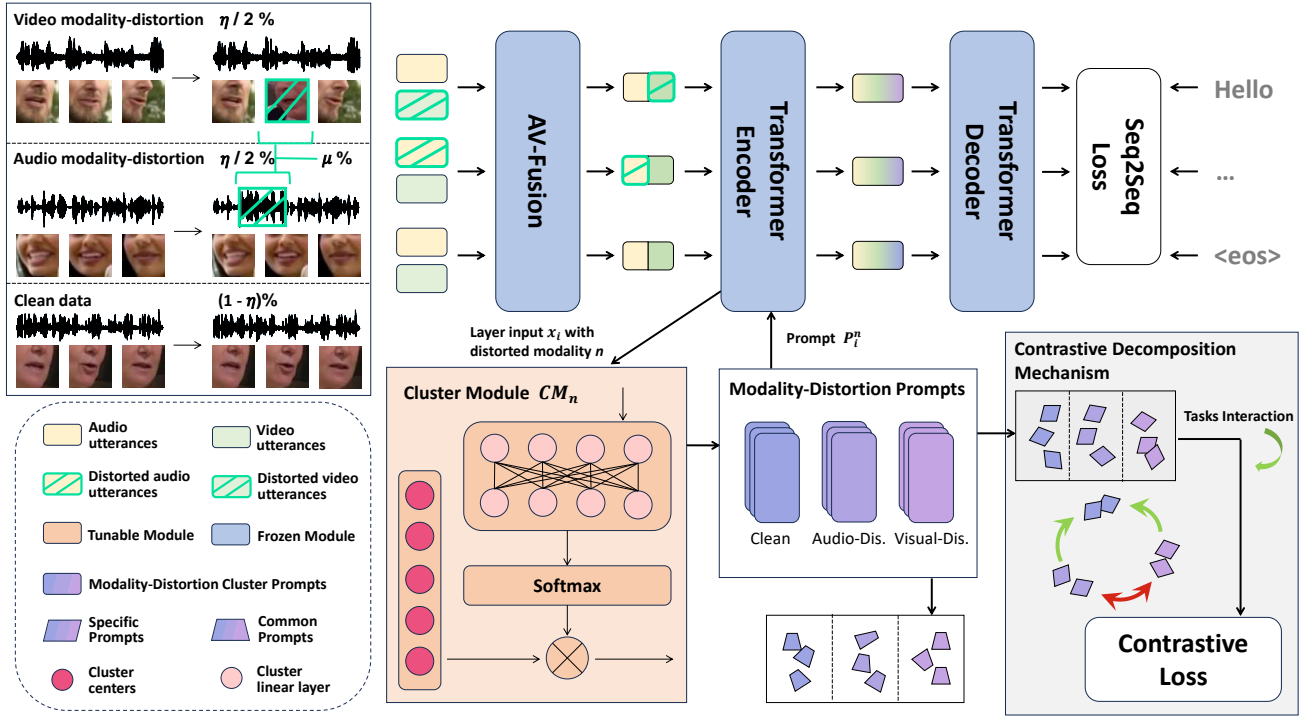


**Figure 2: The overall framework of our proposed PCD approach. Upon pre-training a audio-visual alignment transformer on high-resource dataset, we freeze the structure and finetune the prompts on distorted dataset. Specifically, we train the cluster module  $CM_n$  tailored to data with distorted modality  $n$  to generate bespoke prompts. In addition to the seq2seq loss, a contrastive decomposition mechanism is utilized to supervise the learning of task-specific features in prompts.**

## 3 METHOD

### 3.1 Problem Formulation

We formulate the problem setting for AVSR with modality-distortion in this section. Suppose we have an audio-visual dataset contains modality-distortion  $\tilde{D} = \{\tilde{A}, \tilde{V}, S\}$ , where  $\tilde{A}, \tilde{V}$  represents the audio and video utterance that may be contaminated by random distortion, and  $S$  represents corresponding natural sentence. Neglecting the scenario where distortion concurrently affects both modalities, as explained earlier, we partition the dataset into three subsets: clean data  $D_c = \{A, V, S\}$ , data with audio distortion  $D_{ad} = \{\tilde{A}, V, S\}$ , data with video distortion  $D_{vd} = \{A, \tilde{V}, S\}$ . Under such real-world conditions, there are two challenging problems, one is to adapt one model framework to multiple types of distortion while minimizing computational resources. The other is to avoid confusion from distorted data during the training process.

### 3.2 Transformer with Audio-Visual Alignment

Since AVSR can be viewed as a sequence-to-sequence transformation task, current state-of-the-art AVSR methods are all based on transformer structures. To fully exploit multi-modal knowledge, we employ the audio-visual aligned encoder, similar to AV-Hubert[27], which is a self-supervised representation learning method for audio-visual speech. The AV-Hubert structure integrates and extracts

audio-visual features from raw data, which are then utilized by a transformer decoder to generate natural sentences.

The pre-training process of AV-Hubert alternates between feature clustering and mask prediction. The model leverages clustering to generate self-supervised targets and strengthens cross-modal fusion through mask prediction, facilitating the mapping of audio and video sequences into a unified phoneme space  $f^P \in \mathbb{R}^{T \times D}$  where  $T$  is the length of the sequence and  $D$  is the dimension of the embedding.

Upon acquiring audio-visual representations through self supervised methods, the seq2seq loss is utilized to train the entire model, including the decoder, and also serves as part of the objective for prompt training:

$$\mathcal{L}_{s2s} = - \sum_{t=1}^s \log p(w_t | \{w_i\}_{i=1}^{t-1}, f^P) \quad (1)$$

where  $\{w_i\}_{i=1}^s$  is the ground-truth transcription.

Due to its superior performance on both multi-modal and uni-modal tasks, we choose the AV-Hubert as our backbone model, pre-trained on large-scale vision and audio datasets. Amidst encountering data distortion in one modality, the exceptional performance of AV-Hubert in uni-modality speech recognition facilitates a more effective guidance to prioritize the clean modality. However, the cost of training a full AV-Hubert model to a specific distorted

condition is prohibitive, and practical tasks often involve diverse types of modality-distortion that cannot be addressed by a single model. So we design prompts tailored to different combinations of data distorted on a pre-trained AV-Hubert model to transfer knowledge from a high-resource domain to a low-resource domain with minimal training cost.

### 3.3 Cluster-Prompt for Modality-Distortion

Following pre-training, the subsequent step involves guiding the model to acclimate to distorted data, which often exhibits various types of distortion and is characterized by limited quantity in real-world scenarios. To guide the model pay more attention to the clean part in distortion contaminated audio-visual pairs, we design bespoke prompts for each conditions which are collections of trainable vectors, interacting with the model. Typically, for the tasks set  $N$ , we assign  $|N|$  kinds of prompts where the number is three for training setting simulating real-world modality-distortion scenarios, as formulated in Section 3.1. The corresponding prompts are concatenated to designated positions of the multi-head self-attention (MSA) module.

In the preceding step, we adopt AV-Fusion to map audio and visual representations into the same phoneme space to enable the model to attain recognition capabilities across uni-modality, making it more adept at handling modality-distortion. Initially, the concatenation of audio and visual utterances  $u^{av} = \text{concat}(u^a, u^v) \in \mathbb{R}^{T \times 2D}$  is fed into AV-Fusion to obtain the fused features  $f^m \in \mathbb{R}^{T \times D}$ . Using  $f^m$  as the input to the first layer of the transformer encoder, we denote the input fused features of the  $i$ -th MSA layer as  $x_i \in \mathbb{R}^{T \times D}$ ,  $i = 1, 2, \dots, M$  with number of layers  $M$ . Based on the input distortion type, we choose the respective prompts  $p_i^n \in \mathbb{R}^{L_p \times D}$  with prompt length  $L_p$  and representations for different modality-distortion cases  $n \in N \equiv \{c, ad, vd\}$ , which are then interacted with  $x_i$  to generate extended features  $x_i^p$ :

$$x_i^p = F_{\text{prompt}}(p_i^n, x_i) \quad (2)$$

where  $F_{\text{prompt}}$  defines the attach approaches for prompts to interact with the designated structures in MSA layers.

**3.3.1 Cluster-Based Prompts.** In order to extract valuable features from distorted data, we adopt a cluster strategy for prompt generation. In the pre-training process, a k-means approach is employed to extract cluster labels on audio-visual features. Building upon this concept, we employ an tunable cluster module  $CM_n$  to cluster the inputs with modality-distortion condition  $n$ , thereby generating corresponding prompts. For audio-visual features that exhibits greater similarity, cluster module facilitates prompts in offering more proximate guidance to the pre-trained model. Specifically, the input  $x_i$  is first fed into a extraction network, which is consisted of a linear projection layer, a summation operation and a cluster-wise softmax layer to extract the cluster weights for each phoneme features. We define cluster centers  $c_i \in \mathbb{R}^{N_c \times L_p \times D}$  in each layer  $i$  of the encoder, where  $N_c$  is the number of the clusters and compute prompts by combining them with the clustering results of the input:

$$p_i = \text{Extract}(x_i) \times c_i \quad (3)$$

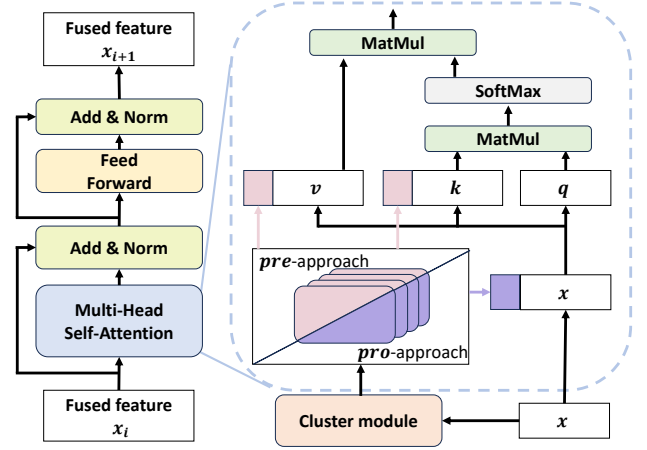


**Figure 3: The illustration of two prompts attach strategies.** After being generated by the cluster module, prompts can be concatenated with the input (*pro-approach*) within the multi-head self-attention (MSA) block, or alternatively, they can be concatenated with the key&value pairs (*pre-approach*).

In the situation of modality-distortion, cluster module strengthens the connections between similar clusters of phoneme features, learning features about the distorted segment.

**3.3.2 Prompt Attach Strategies.** The design of the  $F_{\text{prompt}}$  function, as outlined in Equation 2, is crucial for integrating prompts with pre-trained models to transfer knowledge from a high-quality domain to a target low-quality domain. We adopt two interaction mechanisms with the MSA module, as shown in Fig. 3.

We denote the query, key and value in the  $i$ -th MSA layer as  $Q_i, K_i, V_i$ , which are obtained by applying a projection matrix to  $x_i$ . The first strategy which is inspired by the concept of soft prompt tuning (*Pro*) is to prepend prompts with input sequences for each layer, which is equivalent to concatenate the same prompt parameters to  $Q_i, K_i$  and  $V_i$ . The prompt function can be written as:

$$F_{\text{prompt}}^{\text{Pro}}(p_i^n, x_i) = \text{ATTEN}_i([p_i^n; Q_i], [p_i^n; K_i], [p_i^n; V_i]) \quad (4)$$

where  $[...; ...]$  represents the concatenation operation. With the implementation of *Pro*-approach prompts, attention mechanisms are more targeted towards feature processing, and each layer's input token  $x_i$  contains inherited prompt information from the previous layers, leading to more effective instructions for the model prediction.

Another prompting approach, inspired by prefix tuning (*Pre*), focuses on the key and value at the MSA layer. We split the prompt  $p_i^n$  into two sub-prompts  $p_i^k, p_i^v$  and prepend them to the key and value vectors respectively. We can define the prompt function for *Pre*-approach prompts as:

$$F_{\text{prompt}}^{\text{Pre}}(p_i^n, x_i) = \text{ATTEN}_i(Q_i, [p_i^k; K_i], [p_i^v; V_i]) \quad (5)$$

The attention-level prompting provides another way to instruct the pretrained model from the perspective of the attention mechanism in transformers.

### 3.4 Contrastive Decomposition

To supervise prompt learning for specific modal combinations with distortion, we employ a common-specific decomposition approach. Specifically, we employ a low-rank decomposition mechanism to map the information from  $p^n$  into the common represents  $p_c \in \mathbb{R}^{r \times d}$  and task-specific represents  $p_s^n \in \mathbb{R}^{L_p \times r}$  where  $r$  donates the rank of the matrix decomposition, which can be formulated as:

$$p^n = p_s^n \cdot p_c \quad (6)$$

where  $\cdot$  denotes matrix multiplication. This was done to distinguish between the common features of the AVSR task and the specific characteristics of a particular modality-distortion condition. Rethinking the cluster process, the low-rank decomposition of prompts  $p_i^n$  is equivalent to the same operation applied to cluster centers  $c_i^n$  when implementing.

To constrain the implicit interaction between prompts, we focus on the explicit connections between tasks. We anticipate similar tasks to entail prompts that provide more analogous guidance to the model. In the context of modality-distortion in AVSR, our objective is to attain model performance comparable to clean data even in the presence of audio and video distortion, which means narrowing the gap between prompts in the clean domain  $p_s^c$  and those in the distorted domains  $p_s^{ad}, p_s^{vd}$  while widening the separation between the latter two. Specifically, we propose a contrastive loss following InfoNCE Loss[30] with specific prompt  $p_s^n$  to supervise common-specific decomposition contrastive learning:

$$\mathcal{L}_{cl} = \sum_{n \in N} -\frac{1}{|C(n)|} \sum_{m \in C(n)} \log \frac{\exp \text{sim}(p_s^n, p_s^m) / \tau}{\sum_{k \in N \setminus \{n\}} \exp \text{sim}(p_s^n, p_s^k) / \tau} \quad (7)$$

where  $C(n)$  represents the set of tasks that have a closer relationship to task  $n$  (e.g. when  $n$  refers to the task dealing with data with audio distortion,  $C(n)$  contains the task with clean data),  $|C(n)|$  is its cardinality,  $\tau$  is the temperature parameter, and  $\text{sim}(a, b)$  denotes the similarity between vectors  $a$  and  $b$ . Drawing from an analysis of explicit task relationships, positive and negative sample sets are derived. Contrastive learning is then applied to encourage similar tasks to learn more similar prompts, facilitating the extraction of task-related information and enhancing the effectiveness of guiding the model.

For the overall objective of the prompt training, we apply the  $\mathcal{L}_{cl}$  and cross-entropy loss  $\mathcal{L}_{s2s}$  in Eqn. 1 with the scale factor  $\alpha$ :

$$\mathcal{L}_{overall} = (1 - \alpha)\mathcal{L}_{s2s} + \alpha\mathcal{L}_{cl} \quad (8)$$

## 4 EXPERIMENT

### 4.1 Dataset

*LRS2*. [1] stands out as one of the most widely utilized publicly accessible English lip-reading datasets, including 224 hours of video content sourced from BBC television programs. This dataset originally comprises two partitions for training: Pretrain (195h) and Train (29h), both transcribed at the sentence level from video to text. The key disparity lies in the fact that video clips in the Pretrain partition are not rigorously trimmed and may exceed the corresponding text length. Our experiments on LRS2 involving varying training

data amounts, specifically comparing Pretrain+Train (224h) against Train (29h).

*LRS2-DISTORTED*. Based on the LRS2 dataset, we further propose the LRS2-DISTORTED to verify the robustness to the modality-distortion speech recognition with low-resource training data. We introduce various types of modality-distortion into the LRS2 dataset, aiming to simulate realistic scenarios where audio and visual distortion randomly occurs across both training and testing phases. Note that to ensure fair training, the specific distortion data replaced or added for each sample is predetermined. Meanwhile, both the distortion rate and the distortion types can be varied to compare the robustness of the models.

### 4.2 Metric

For all experiments we use the word error rate (WER) as the evaluation index of speech recognition. WER can be defined a  $WER = (S + D + I)/M$ , where  $S, D, I, M$  represent the number of words replaced, deleted, inserted and referenced respectively.

### 4.3 Implementation Details

**4.3.1 Modality-Distortion Setting.** We focus on a more practical scenario where distortion is prevalent both in training and testing phases. We define distortion rate  $\eta$  as the proportion of modality-distortion data to the entire dataset, and  $\mu$  as the proportion of distortion present in each individual sample. Scenario with distortion rate  $\eta$  and  $\mu$  indicates that there are  $\eta/2$  data with audio distortion,  $\eta/2$  data with video distortion, and  $(1 - \eta)$  complete data, where  $\mu$  of each sample is replaced by data with distortion. To validate the robustness of the method, we employ three approaches to simulate distortion. Approach *a* simulates a severe scenario entailing replacing segments of either the audio or video with segments from another sample, and Approach *b* involved adding MUSAN [29] noise to the audio and introducing screen flickering to the video. Approach *c* represents temporal asynchrony between audio and video, a prevalent type of distortion in real-world scenarios. Specifically, it entails delaying the data of the distortion modality by a specified number of frames. In ablation experiments, we default to setting  $\eta = 70\%$ ,  $\mu = 80\%$  for inference with condition *a*.

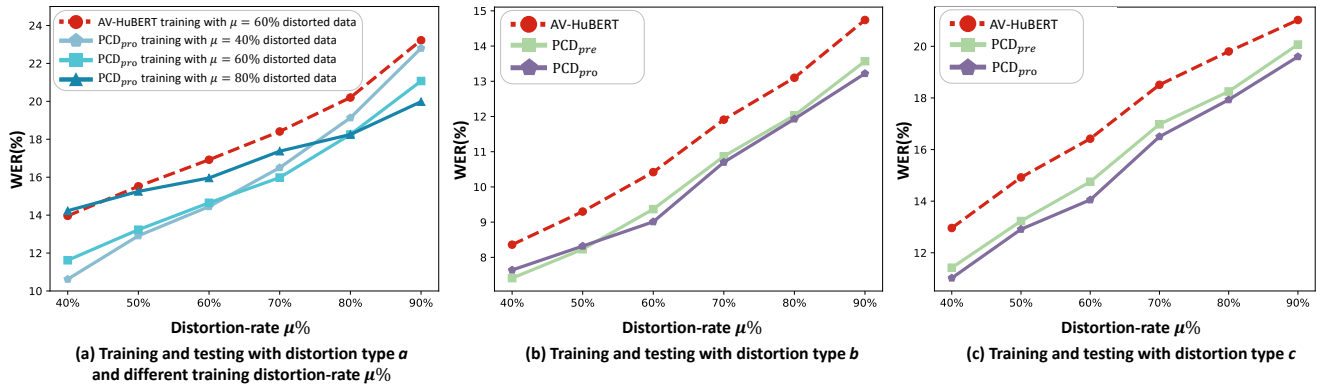
**4.3.2 Experimental Details .** The model is trained on NVIDIA GeForce RTX 3080Ti GPU, equipped with 10GB of VRAM. Constrained by computational resources and the simulation of low-resource data, we conduct ablation experiments mainly on the base transformer model on the LRS2-29h dataset.

### 4.4 Main Result

In this section, we compare the performance of our approach with the backbone and other AVSR methods under modality-distortion setting on LRS2, as presented in Table 1. Limited by data distortion, the performance of these baselines deviates significantly from the result training with clean data, indicating the lack of robustness to modality-distortion. Comparatively, our proposed PCD outperforms the state-of-the-art AVSR across various distortion settings, achieving significant reductions in the metric (up to 3% on WER) compared to the backbone, AV-Hubert. It is noteworthy that all improvements are derived from approximately 2% of the parameters

**Table 1: The WER (%) performance on LRS2-DISTORTED under the modality-distortion AVSR setting under different evaluating distortion rates with distortion approach *a*. Models are trained under  $\eta = 70\%$ ,  $\mu = 60\%$ .**

model	training set	clean	$\eta=50\%$		$\eta=70\%$		$\eta=90\%$		
			$\mu=60\%$	$\mu=80\%$	$\mu=60\%$	$\mu=80\%$	$\mu=60\%$	$\mu=80\%$	
TM-Seq2seq [1]		12.20	25.26	28.63	32.85	37.44	39.71	46.51	
End2end Conformer [20]	224h-distorted	6.13	13.12	15.97	14.92	19.89	19.78	24.32	
LUSL-AVSR [22]		4.95	10.73	12.76	13.98	16.53	17.01	21.29	
Auto-AVSR [19]		4.01	10.41	11.98	12.63	15.20	16.31	19.23	
AV-HuBERT		6.81	14.22	16.71	16.92	20.20	20.18	24.47	
transformer-base	PCD <sub>pre</sub>	29h-distorted	<b>5.56</b>	<b>11.79</b>	14.70	<b>14.65</b>	18.90	17.28	22.91
	PCD <sub>pro</sub>	29h-distorted	5.73	11.82	<b>14.51</b>	14.79	<b>18.25</b>	<b>17.12</b>	<b>22.12</b>
	AV-HuBERT	224h-distorted	4.36	10.56	12.60	12.83	15.83	17.04	19.43
PCD <sub>pre</sub>	224h-distorted	<b>3.89</b>	<b>9.32</b>	11.43	11.52	14.79	15.89	18.11	
PCD <sub>pro</sub>		3.95	9.61	<b>11.38</b>	<b>11.47</b>	<b>14.41</b>	<b>15.65</b>	<b>17.93</b>	
transformer-large	AV-HuBERT	29h-distorted	5.69	11.29	14.45	13.71	18.40	16.13	22.18
	PCD <sub>pre</sub>	29h-distorted	<b>4.78</b>	<b>9.51</b>	13.12	12.31	16.80	14.21	20.48
	PCD <sub>pro</sub>	29h-distorted	4.80	9.81	<b>12.54</b>	<b>12.19</b>	<b>16.44</b>	<b>13.89</b>	<b>19.56</b>
	AV-HuBERT	224h-distorted	3.54	8.13	10.71	10.23	14.20	11.77	16.44
	PCD <sub>pre</sub>	224h-distorted	<b>3.28</b>	<b>7.04</b>	9.82	9.13	13.51	9.95	14.78
	PCD <sub>pro</sub>	224h-distorted	3.32	7.23	<b>9.53</b>	<b>8.99</b>	<b>13.12</b>	<b>9.83</b>	<b>14.21</b>

**Figure 4: Performance of PCD under different training distortion rates and its behavior under various distortion conditions.**

of AV-HuBERT. The poor performance of the baselines is attributed to their focus on utilizing complete modalities, leading to inadequate adaptation to modality-distortion scenarios. In contrast, benefiting from the prompts designed for various distortion conditions, PCD learns how to leverage pre-trained comprehensive knowledge to tackle different situations. The cluster-prompt module offers a robust instructional framework for guiding model predictions. Moreover, the contrastive decomposition constraint enhances the interaction between prompts, while learning task-specific features strengthens the robustness to distortion settings. The main results convincingly illustrate the effectiveness of our proposed method.

From the perspective of distortion settings, as the distortion rate  $\eta$  increases, the magnitude of improvement consistently rises, indicating that PCD's guidance on distorted samples is stronger than on clean data. PCD also demonstrates greater robustness to varying distortion rates  $\mu$ , with a corresponding increase in improvement.

From the perspective of model strategy analysis, the *pre*-approach demonstrates superior performance under low-distortion settings, whereas the ability of *pro*-approach to convey information across different layers renders it more suitable for high-distortion data. From a data quantity perspective, it is observed that PCD exhibits a more significant enhancement on the 29h dataset than 224h since sufficient data has enabled the backbone to acquire more knowledge and adapt to the distortion settings. In other words, PCD not only ensures stable improvements over 224h dataset but also demonstrates greater suitability for low-quality target domains, which aligns with the primary application scenario proposed.

## 4.5 Ablation study

**4.5.1 Robustness to different distortion setting.** In the main result, we validate the robustness of the PCD method to varying distortion rates during the testing phase with distortion type *a*.

In this section, we conduct additional experiments to explore the performance of PCD under different training distortion rates and its behavior under various distortion conditions. In Figure 4 (a), we test the performance of models trained under different distortion rates  $\mu$ . Typically, using data with lower distortion rates allows the model to acquire more knowledge, as evident from the test results under a 40% distortion rate. However, models trained with too little distortion are not adept at tasks with excessively high distortion rates. Moderate levels of distortion can aid in improving the model's generalization ability. Based on this, we select the model trained under the 60% distortion condition, which exhibit the optimal trade-off metric. In Figure 4 (b, c), while keeping other settings constant, we conduct a comparison between PCD and the baseline under the additional distortion settings  $b, c$  mentioned in section 4.3.1. It can be observed that the PCD method exhibits improvements when confronted with different real-world distortion scenarios and robustness across varying distortion rates.

**4.5.2 The Impact of cluster center.** The Cluster Prompt module implicitly learns distinct features of the modality-distortion by distinguishing between different phoneme features, enabling the model to provide targeted prompts. In Figure 5, we show the influence of the number of clusters on the performance of accuracy. In contrast to abstaining from the cluster strategy (i.e., with zero cluster centers), the cluster module affords the model a degree of flexibility in addressing the modality-distortion, consequently enhancing recognition accuracy. The optimal performance under the 29h dataset is achieved with 30 cluster centers, whereas the number is 80 for the 224h dataset. This indicates that a higher number of cluster centers represent a finer handling of distorted data. But excessive cluster centers result in insufficient data to adequately train these parameters, leading to a decline in recognition performance.

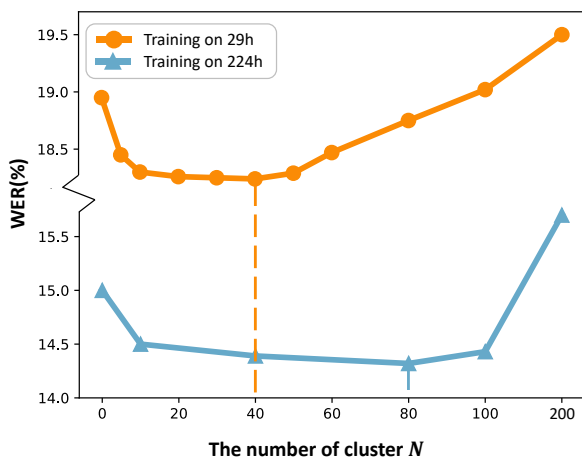


**Figure 5: Comparison of  $PCD_{pro}$  performance with different number of clusters ( $N$ ).**

**4.5.3 The Impact of prompt length.** We conduct experiments to investigate the impact of prompt length on accuracy in Figure 5. Similar to the results with cluster center numbers, initially, as

the prompt length increases, it provides more information for the model, resulting in improved accuracy. However, beyond a certain point, the data becomes insufficient to train the corresponding parameters, leading to a decline in recognition capability. It is noteworthy that the inflection points obtained from the prompt method and the prefix method are different. This discrepancy arises because the prompt tuning method directly concatenates the prompt with the input, resulting in an increasing length of input at each layer. Consequently, excessively long prompts adversely affect the input.

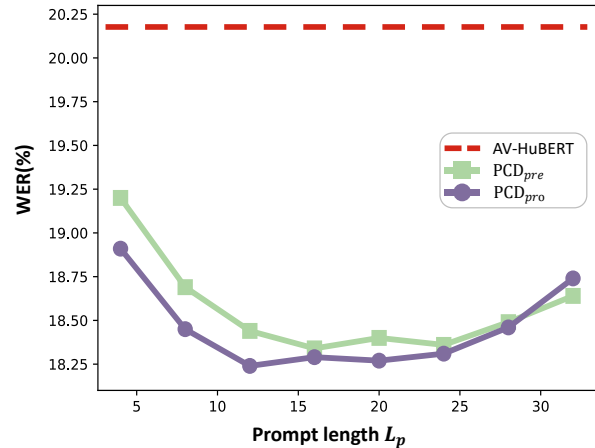


**Figure 6: Comparison of PCD performance with different prompt length ( $L_p$ ).**

**4.5.4 The Impact of Contrastive Decomposition.** In our proposed method, a contrastive decomposition framework is designed to constrain the generation of prompts. We investigate the impact of the framework as shown in Table 2. Compared to the scenario without using the framework (i.e.,  $\alpha = 0$ ), employing contrastive decomposition loss as a regularization term can effectively enhance the model's recognition accuracy. It enables the prompts to learn task-specific features and makes the model performance under modality-distortion closer to clean data. However, an excessive weighting of the contrastive loss may impede the model's learning of recognition capabilities. When the prompts themselves have not acquired sufficient knowledge, increasing constraints would be meaningless.

**Table 2: Parameter sensitivity of  $PCD_{pro}$  to different setting of contrastive decomposition framework.**

Models	$\alpha$	Wer (%)
AV-Hubert	-	20.20
	0	18.83
$PCD_{pro}$	0.001	18.78
	0.01	<b>18.25</b>
	0.1	20.01

**4.5.5 Testing under extremely harsh conditions.** In handling the data with distortion, given the challenges in recognition and high distortion rates, we choose to discard scenarios where both modalities are distorted. However, this data may also be useful in practice. In this section, we investigate the performance of PCD in extremely harsh environments, where distortion can randomly occur in both modalities, as shown in Table 3. Apart from setting both modalities to have distortion to replace clean data, all other settings remain consistent, including adjusting the contrastive decomposition module to bring the specific-prompt for scenarios with both distorted modalities closer to those under single-modality distortion. As a result, PCD still brings improvements to model recognition accuracy. These improvements stem from the guidance on recognizing single-modal distorted data and the enhanced contextual understanding of recognizing multi-modal distorted data.

**Table 3: WER (%) performance of PCD in extreme harsh conditions. dis. represents distorted**

Models	training set	$\eta=90\%$		$\eta=70\%$	
		$\mu=20\%$	$\mu=40\%$	$\mu=20\%$	$\mu=40\%$
AV-Hubert	29h-clean	21.13	35.24	25.04	39.43
AV-Hubert	29h-dis.	14.20	21.76	16.73	25.49
PCD <sub>pre</sub>	29h-dis.	13.40	20.12	15.14	24.54
PCD <sub>pro</sub>	29h-dis.	<b>13.23</b>	<b>19.13</b>	<b>15.01</b>	<b>23.07</b>

**4.5.6 Comparison with the missing modality.** Since distortion can impact model recognition, an obvious question arises: can we simply discard the modality-distortion to address the missing modality problem? Missing modality is another research hotspot in the multi-modal field, but similarly, there is no method that simultaneously addresses the presence of multiple missing conditions in the context of AVSR. We also evaluate PCD’s performance with missing modality and compare it with distorted modality, presenting the results in Figure 7. When focusing on the missing scenarios in the left half of the image, we observe that PCD exhibits improvements across all levels of missing, particularly enhancing performance by 2.8% when the missing rate is at 100%. When considering the comparison between missing and distorted data across the entire figure, we observe that when samples are completely covered by distorted data, discarding the distorted modality entirely is a viable option. However, when the distortion covers only 80% or less of the samples, employing PCD leads to better results. The results demonstrate that the PCD method effectively guides the model not only in distortion settings but also in missing scenarios.

**4.5.7 Enhancement for existing models.** Some outstanding AVSR approaches achieve high-precision recognition on clean data, yet this very attribute renders them highly susceptible to interference from fake segments. Since PCD involves adding an additional prompt module to a frozen model, we fine-tune the pre-trained AVHubert on the LRS3-distorted to improve the model’s robustness to distortion while retaining its original performance, and the results are displayed in Table 4. Models trained on clean data exhibit poor performance when confronting modality-distortion.

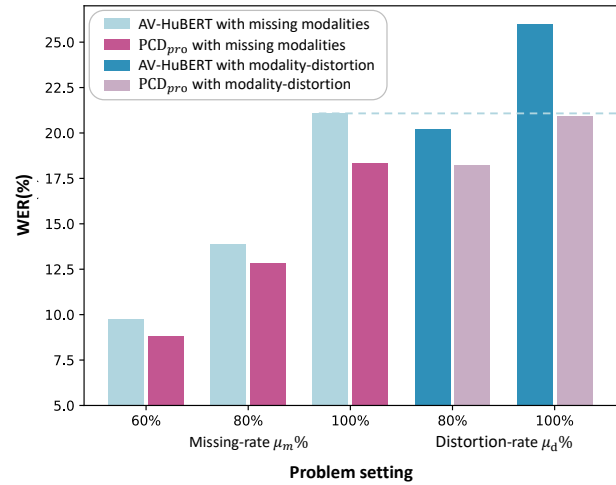


**Figure 7: The experimental results on missing modality and comparison with modality-distortion.**

Moreover, fine-tuning on distorted data notably impacts the original performance of the model on clean data. In contrast, models optimized with PCD, which only train a few parameters, greatly enhance the model’s robustness to modality-distortion. Due to the considerable reduction in training data, there is a slight decrease in performance on clean data.

**Table 4: Comparison between existing models and PCD-optimized models on LRS3 dataset. dis. represents distorted**

Models	training set	Param (MB)	$\eta = 70\%$ Wer(%)		
			$\mu=0\%$	$\mu=60\%$	$\mu=80\%$
AV-Hubert	30h-clean	161.5	<b>4.08</b>	29.32	39.04
AV-Hubert	30h-dis.	161.5	6.58	18.23	20.89
PCD <sub>pre</sub>	30h-dis.	3.84	4.10	17.13	19.22
PCD <sub>pro</sub>	30h-dis.	3.84	4.13	<b>16.74</b>	<b>18.83</b>
AV-Hubert	433h-clean	161.5	<b>1.83</b>	30.88	38.90
AV-Hubert	433h-dis.	161.5	5.10	15.96	19.65
PCD <sub>pre</sub>	433h-dis.	3.84	1.94	14.00	16.92
PCD <sub>pro</sub>	433h-dis.	3.84	1.99	<b>13.92</b>	<b>16.78</b>

## 5 CONCLUSION

In this paper, we have proposed a novel method called PCD aiming to enhance robustness to modality-distortion in AVSR task. Concretely, we introduce prompt learning and design specific prompts for each type of modality-distortion to guide the model in adapting to the distortion. In order to effectively transfer knowledge from the high-quality domain obtained through pre-training to the low-quality domain with distortion, we employ two cluster-prompt strategies. In addition, to better fit task-specific features into prompts, we design a contrastive learning mechanism to constrain the generation of prompts. Extensive results on the newly-created benchmarks of modality-distortion speech recognition illustrates the superiority of our proposed method.



## REFERENCES

- [1] Triantafyllos Afouras, Joon Son Chung, Andrew Senior, Oriol Vinyals, and Andrew Senior. 2018. Deep audio-visual speech recognition. *IEEE transactions on pattern analysis and machine intelligence* 44, 12 (2018), 8717–8727.
- [2] Mohamed Sami Anwar, Bowen Shi, Vedanuj Goswami, Wei-Ning Hsu, Juan Miguel Pino, and Changhan Wang. 2023. MuAViC: A Multilingual Audio-Visual Corpus for Robust Speech Recognition and Robust Speech-to-Text Translation. *ArXiv abs/2303.00628* (2023). <https://api.semanticscholar.org/CorpusID:257255284>
- [3] Oscar Chang, Otavio Braga, Hank Liao, Dmitriy Serdyuk, and Olivier Siohan. 2023. On Robustness to Missing Video for Audiovisual Speech Recognition. *arXiv:2312.10088* [eess.AS]
- [4] Yusheng Dai, Hang Chen, Jun Du, Ruoyu Wang, Shihao Chen, Jiefeng Ma, Haotian Wang, and Chin-Hui Lee. 2024. A Study of Dropout-Induced Modality Bias on Robustness to Missing Video Frames for Audio-Visual Speech Recognition. *arXiv:2403.04245* [cs.SD]
- [5] Adriana Fernandez-Lopez, Honglie Chen, Pingchuan Ma, Alexandros Haliassos, Stavros Petridis, and Maja Pantic. 2023. SparseVSR: Lightweight and Noise Robust Visual Speech Recognition. *ArXiv abs/2307.04552* (2023). <https://api.semanticscholar.org/CorpusID:259501735>
- [6] Tianyu Gao, Adam Fisch, and Danqi Chen. 2021. Making Pre-trained Language Models Better Few-shot Learners. In *Proceedings of the 59th Annual Meeting of the Association for Computational Linguistics and the 11th International Joint Conference on Natural Language Processing (Volume 1: Long Papers)*, Chengqing Zong, Fei Xia, Wenjie Li, and Roberto Navigli (Eds.). Association for Computational Linguistics, Online, 3816–3830. <https://doi.org/10.18653/v1/2021.acl-long.295>
- [7] Anmol Gulati, James Qin, Chung-Cheng Chiu, Niki Parmar, Yu Zhang, Jiahui Yu, Wei Han, Shibo Wang, Zhengdong Zhang, Yonghui Wu, et al. 2020. Conformer: Convolution-augmented transformer for speech recognition. *arXiv preprint arXiv:2005.08100* (2020).
- [8] Xu Han, Weilin Zhao, Ning Ding, Zhiyuan Liu, and Maosong Sun. 2021. PTR: Prompt Tuning with Rules for Text Classification. *arXiv:2105.11259* [cs.CL]
- [9] Joanna Hong, Minsu Kim, Jeongsoo Choi, and Yong Man Ro. 2023. Watch or Listen: Robust Audio-Visual Speech Recognition with Visual Corruption Modeling and Reliability Scoring. *arXiv:2303.08536* [cs.MM]
- [10] Yuchen Hu, Ruizhe Li, Cheng Chen, Chengwei Qin, Qiu shi Zhu, and Eng Siong Chng. 2023. Hearing Lips in Noise: Universal Viseme-Phoneme Mapping and Transfer for Robust Audio-Visual Speech Recognition. In *Annual Meeting of the Association for Computational Linguistics*. <https://api.semanticscholar.org/CorpusID:259202515>
- [11] Rongjie Huang, Jiawei Huang, Dongchao Yang, Yi Ren, Luping Liu, Mingze Li, Zhenhui Ye, Jinglin Liu, Xiang Yin, and Zhou Zhao. 2023. Make-An-Audio: Text-To-Audio Generation with Prompt-Enhanced Diffusion Models. *arXiv:2301.12661* [cs.SD]
- [12] Menglin Jia, Luming Tang, Bor-Chun Chen, Claire Cardie, Serge Belongie, Bharath Hariharan, and Ser-Nam Lim. 2022. Visual Prompt Tuning. *arXiv:2203.12119* [cs.CV]
- [13] Muhammad Uzair Khattak, Hanoona Rasheed, Muhammad Maaz, Salman Khan, and Fahad Shahbaz Khan. 2023. MaPLE: Multi-modal Prompt Learning. *arXiv:2210.03117* [cs.CV]
- [14] Brian Lester, Rami Al-Rfou, and Noah Constant. 2021. The Power of Scale for Parameter-Efficient Prompt Tuning. *arXiv:2104.08691* [cs.CL]
- [15] Xiang Lisa Li and Percy Liang. 2021. Prefix-Tuning: Optimizing Continuous Prompts for Generation. *arXiv:2101.00190* [cs.CL]
- [16] Zhengyang Li, Chenwei Liang, Timo Lohrenz, Marvin Sach, Björn Möller, and Tim Fingscheidt. 2023. An Efficient and Noise-Robust Audiovisual Encoder for Audiovisual Speech Recognition. In *Proc. INTERSPEECH 2023*. 1583–1587. <https://doi.org/10.21437/Interspeech.2023-793>
- [17] Hong Liu, Wenhao Li, and Bing Yang. 2021. Robust Audio-Visual Speech Recognition Based on Hybrid Fusion. In *2020 25th International Conference on Pattern Recognition (ICPR)*. 7580–7586. <https://doi.org/10.1109/ICPR48806.2021.9412817>
- [18] Pengfei Liu, Weizhe Yuan, Jinlan Fu, Zhengbao Jiang, Hiroaki Hayashi, and Graham Neubig. 2021. Pre-train, Prompt, and Predict: A Systematic Survey of Prompting Methods in Natural Language Processing. *arXiv:2107.13586* [cs.CL]
- [19] Pingchuan Ma, Alexandros Haliassos, Adriana Fernandez-Lopez, Honglie Chen, Stavros Petridis, and Maja Pantic. 2023. Auto-AVSR: Audio-Visual Speech Recognition with Automatic Labels. *ICASSP 2023 - 2023 IEEE International Conference on Acoustics, Speech and Signal Processing (ICASSP)* (2023), 1–5. <https://api.semanticscholar.org/CorpusID:257767381>
- [20] Pingchuan Ma, Stavros Petridis, and Maja Pantic. 2021. End-to-end audio-visual speech recognition with conformers. In *ICASSP 2021-2021 IEEE International Conference on Acoustics, Speech and Signal Processing (ICASSP)*. IEEE, 7613–7617.
- [21] Takaki Makino, Hank Liao, Yannis Assael, Brendan Shillingford, Basilio Garcia, Otavio Braga, and Olivier Siohan. 2019. Recurrent Neural Network Transducer for Audio-Visual Speech Recognition. *arXiv:1911.04890* [eess.AS]
- [22] Xichen Pan, Peiyu Chen, Yichen Gong, Helong Zhou, Xinbing Wang, and Zhouhan Lin. 2022. Leveraging Unimodal Self-Supervised Learning for Multi-modal Audio-Visual Speech Recognition. *arXiv:2203.07996* [cs.SD]
- [23] Stavros Petridis, Themos Stafylakis, Pingchuan Ma, Georgios Tzimiropoulos, and Maja Pantic. 2018. Audio-Visual Speech Recognition With A Hybrid CTC/Attention Architecture. *arXiv:1810.00108* [cs.CV]
- [24] Zi Qian, Xin Wang, Xuguang Duan, Pengda Qin, Yuhong Li, and Wenwu Zhu. 2023. Decouple Before Interact: Multi-Modal Prompt Learning for Continual Visual Question Answering. In *2023 IEEE/CVF International Conference on Computer Vision (ICCV)*. 2941–2950. <https://doi.org/10.1109/ICCV51070.2023.00276>
- [25] Kuniaki Saito, Kihyuk Sohn, Xiang Zhang, Chun-Liang Li, Chen-Yu Lee, Kate Saenko, and Tomas Pfister. 2023. Prefix Conditioning Unifies Language and Label Supervision. *arXiv:2206.01125* [cs.CV]
- [26] Dmitriy Serdyuk, Otavio Braga, and Olivier Siohan. 2022. Transformer-Based Video Front-Ends for Audio-Visual Speech Recognition for Single and Multi-Person Video. *arXiv:2201.10439* [cs.CV]
- [27] Bowen Shi, Wei-Ning Hsu, Kushal Lakhotia, and Abdelrahman Mohamed. 2022. Learning Audio-Visual Speech Representation by Masked Multimodal Cluster Prediction. *arXiv:2201.02184* [eess.AS]
- [28] Bowen Shi, Wei-Ning Hsu, and Abdelrahman Mohamed. 2022. Robust self-supervised audio-visual speech recognition. *arXiv preprint arXiv:2201.01763* (2022).
- [29] David Snyder, Guoguo Chen, and Daniel Povey. 2015. MUSAN: A Music, Speech, and Noise Corpus. *arXiv:1510.08484* *arXiv:1510.08484v1*.
- [30] Aaron van den Oord, Yazhe Li, and Oriol Vinyals. 2019. Representation Learning with Contrastive Predictive Coding. *arXiv:1807.03748* [cs.LG]
- [31] Tu Vu, Brian Lester, Noah Constant, Rami Al-Rfou, and Daniel Cer. 2022. SPoT: Better Frozen Model Adaptation through Soft Prompt Transfer. *arXiv:2110.07904* [cs.CL]
- [32] Apoorv Vyas, Bowen Shi, Matthew Le, Andros Tjandra, Yi-Chiao Wu, Baishan Guo, Jiemin Zhang, Xinyue Zhang, Robert Adkins, William Ngan, Jeff Wang, Ivan Cruz, Bapi Akula, Akinniyi Akinyemi, Brian Ellis, Rashel Moritz, Yael Yungster, Alice Rakotoarison, Liang Tan, Chris Summers, Carleigh Wood, Joshua Lane, Mary Williamson, and Wei-Ning Hsu. 2023. Audiobox: Unified Audio Generation with Natural Language Prompts. *arXiv:2312.15821* [cs.SD]
- [33] Zifeng Wang, Zizhao Zhang, Chen-Yu Lee, Han Zhang, Ruoxi Sun, Xiaoqi Ren, Guolong Su, Vincent Perot, Jennifer Dy, and Tomas Pfister. 2022. Learning to Prompt for Continual Learning. *arXiv:2112.08654* [cs.LG]
- [34] Felix Weninger, Hakan Erdogan, Shinji Watanabe, Emmanuel Vincent, Jonathan Roux, John R. Hershey, and Björn Schuller. 2015. Speech Enhancement with LSTM Recurrent Neural Networks and its Application to Noise-Robust ASR. In *Proceedings of the 12th International Conference on Latent Variable Analysis and Signal Separation - Volume 9237 (Liberec, Czech Republic) (LVA/ICA 2015)*. Springer-Verlag, Berlin, Heidelberg, 91–99. [https://doi.org/10.1007/978-3-319-22482-4\\_11](https://doi.org/10.1007/978-3-319-22482-4_11)
- [35] Yi Xin, Junlong Du, Qiang Wang, Ke Yan, and Shouhong Ding. 2023. MmAP: Multi-modal Alignment Prompt for Cross-domain Multi-task Learning. *arXiv:2312.08636* [cs.CV]
- [36] Sheng Yang, Zheng Gong, and Jiancang Kang. 2023. An Improved End-to-End Audio-Visual Speech Recognition Model. *INTER\_SPEECH 2023* (2023). <https://api.semanticscholar.org/CorpusID:260908510>
- [37] Yuan Yao, Bowen Dong, Ao Zhang, Zhengyan Zhang, Ruobing Xie, Zhiyuan Liu, Leyu Lin, Maosong Sun, and Jianyong Wang. 2022. Prompt Tuning for Discriminative Pre-trained Language Models. *arXiv:2205.11166* [cs.CL]
- [38] Kaiyang Zhou, Jingkang Yang, Chen Change Loy, and Ziwei Liu. 2022. Conditional Prompt Learning for Vision-Language Models. *arXiv:2203.05557* [cs.CV]
- [39] Kaiyang Zhou, Jingkang Yang, Chen Change Loy, and Ziwei Liu. 2022. Learning to Prompt for Vision-Language Models. *International Journal of Computer Vision* 130, 9 (July 2022), 2337–2348. <https://doi.org/10.1007/s11263-022-01653-1>
- [40] Jiawen Zhu, Simiao Lai, Xin Chen, Dong Wang, and Huchuan Lu. 2023. Visual Prompt Multi-Modal Tracking. *arXiv:2303.10826* [cs.CV]

929  
930  
931  
932  
933  
934  
935  
936  
937  
938  
939  
940  
941  
942  
943  
944  
945  
946  
947  
948  
949  
950  
951  
952  
953  
954  
955  
956  
957  
958  
959  
960  
961  
962  
963  
964  
965  
966  
967  
968  
969  
970  
971  
972  
973  
974  
975  
976  
977  
978  
979  
980  
981  
982  
983  
984  
985  
986987  
988  
989  
990  
991  
992  
993  
994  
995  
996  
997  
998  
999  
1000  
1001  
1002  
1003  
1004  
1005  
1006  
1007  
1008  
1009  
1010  
1011  
1012  
1013  
1014  
1015  
1016  
1017  
1018  
1019  
1020  
1021  
1022  
1023  
1024  
1025  
1026  
1027  
1028  
1029  
1030  
1031  
1032  
1033  
1034  
1035  
1036  
1037  
1038  
1039  
1040  
1041  
1042  
1043  
1044